Bidirectional regulation of Aβ levels by Presenilin 1

Victor Bustos[a,1], Maria V. Pulina[a], Yildiz Kelahmetoglu[a,2], Subhash C. Sinha[a], Fred S. Gorelick[b,c], Marc Flajolet[a], and Paul Greengard[a,1]

[a]Laboratory of Molecular and Cellular Neuroscience, The Rockefeller University, New York, NY 10065; [b]Department of Internal Medicine, Yale University School of Medicine, New Haven, CT 06520; and [c]Department of Cell Biology, Yale University School of Medicine, New Haven, CT 06520

Contributed by Paul Greengard, April 27, 2017 (sent for review March 30, 2017; reviewed by Yue-Ming Li and Sangram S. Sisodia)

Alzheimer's disease (AD) is characterized by accumulation of the β-amyloid peptide (Aβ), which is generated through sequential proteolysis of the amyloid precursor protein (APP), first by the action of β-secretase, generating the β-C-terminal fragment (βCTF), and then by the Presenilin 1 (PS1) enzyme in the γ-secretase complex, generating Aβ. γ-Secretase is an intramembranous protein complex composed of Aph1, Pen2, Nicastrin, and Presenilin 1. Although it has a central role in the pathogenesis of AD, knowledge of the mechanisms that regulate PS1 function is limited. Here, we show that phosphorylation of PS1 at Ser367 does not affect γ-secretase activity, but has a dramatic effect on Aβ levels in vivo. We identified CK1γ2 as the endogenous kinase responsible for the phosphorylation of PS1 at Ser367. Inhibition of CK1γ leads to a decrease in PS1 Ser367 phosphorylation and an increase in Aβ levels in cultured cells. Transgenic mice in which Ser367 of PS1 was mutated to Ala, show dramatic increases in Aβ peptide and in βCTF levels in vivo. Finally, we show that this mutation impairs the autophagic degradation of βCTF, resulting in its accumulation and increased levels of Aβ peptide and plaque load in the brain. Our results demonstrate that PS1 regulates Aβ levels by a unique bifunctional mechanism. In addition to its known role as the catalytic subunit of the γ-secretase complex, selective phosphorylation of PS1 on Ser367 also decreases Aβ levels by increasing βCTF degradation through autophagy. Elucidation of the mechanism by which PS1 regulates βCTF degradation may aid in the development of potential therapies for Alzheimer's disease.

Presenilin 1 | phosphorylation | Alzheimer's disease | Aβ | autophagy

Alzheimer's disease (AD) is a progressive neurodegenerative disorder characterized by the accumulation of Aβ plaques and neurofibrillary tangles in the brain. Although the disease etiology is not fully understood, patients with inherited early-onset AD have mutations in genes involved in proteolytic generation of Aβ, suggesting a key role for Aβ in disease pathogenesis (1).

Aβ is generated through sequential proteolysis of the amyloid precursor protein (APP), first by β-secretase, producing βCTF, and then by the γ-secretase complex, generating Aβ (2, 3). γ-Secretase is an intramembranous aspartyl protease complex composed of Aph1, Pen2, Nicastrin, and PS1 or PS2. The PS1 isoform has a pivotal role in the pathogenesis of Alzheimer's disease. Although knowledge of its regulation is limited, PS1 phosphorylation can affect its function. For example, PS1 phosphorylation at Ser353 and Ser357 by GSK3β modulates its binding to β-catenin (4). Phosphorylation of PS1 at Ser397 by GSK3β and at Thr354 by P35/Cdk5 regulates PS1 C-terminal fragment stability (5). PS1 phosphorylation at Ser346 by PKC inhibits proteolytic processing of PS1 by caspase activity, thereby reducing the progression of apoptosis (6). Recently, phosphorylation of Ser19 in PS2 was shown to regulate PS2 localization to the late endosome/lysosome (7). PS1 is also phosphorylated on its third intracellular loop at Ser367 (8), but the consequences of this modification or the responsible kinase are unknown.

Here, we report that PS1 phosphorylated at residue Ser367 decreases levels of βCTF, the precursor of Aβ, by increasing its degradation through autophagy. We identified CK1γ as the endogenous protein kinase responsible for phosphorylation of PS1 at Ser367. Transgenic mice in which PS1-Ser367 was mutated to Ala showed dramatic increases in the levels of βCTF and its proteolytic product, Aβ, in vivo. The brains of PS1-S367A knock-in mice show increased levels of LC3-II and SQSMT1/p62 proteins, indicating impaired autophagic flux. We conclude that PS1 regulates Aβ levels in a bidirectional manner. Thus, in addition to the known proamyloidogenic role of PS1 as the catalytic subunit of the γ-secretase complex that processes βCTF to produce Aβ, selective phosphorylation of PS1 on Ser367 results in an antiamyloidogenic function that decreases Aβ levels by increasing βCTF degradation through autophagy.

Results

CK1γ Phosphorylates PS1 at Ser367. We first identified the endogenous kinase responsible for phosphorylating PS1 at Ser367. In silico analysis indicated that Ser367 belongs to a conserved phosphorylation motif recognized by casein kinase 1 (CK1) (9), a protein kinase family with six isoforms: CK1α, CK1γ1, CK1γ2, CK1γ3, CK1δ, and CK1ε. Using systematic knockdown of each CK1 isoform, CK1γ2 was identified as the endogenous kinase most able to phosphorylate PS1 at Ser367 (Fig. 1 *A*–*C*). To confirm these results, we incubated N2A cells with CK1 inhibitors that targeted specific isoforms. Treatment of N2A cells with 2-((4-(2-hydroxypropan-2-yl)phenyl)amino)-1*H*-benzo[*d*]imidazole-6-carbonitrile (HPB), a recently developed CK1γ inhibitor (10), led to a 57% decrease in PS1 pSer367 (Fig. 1 *D* and *E*). Additionally, overexpression of CK1γ2 in mouse fibroblasts induced a 49% increase in phosphorylation of PS1 at Ser367 (Fig. 1 *F* and *G*).

Significance

Alzheimer's disease is the most common neurodegenerative disorder, affecting more than 5 million people in the United States. Multiple lines of evidence suggest that the accumulation of toxic oligomers and aggregates of β-amyloid (Aβ) peptide are the primary causes of neurodegeneration. Aβ originates from sequential cleavage of the amyloid precursor protein (APP). The APP first cleavage is by β-secretase and yields β-C-terminal fragment (βCTF). In turn, βCTF is cleaved by Presenilin 1 (PS1) to produce Aβ. In this work, we show that PS1, in addition to generating Aβ, can also decrease Aβ levels by directing βCTF degradation through autophagy. This previously unrecognized mechanism of regulation of Aβ by Presenilin 1 could provide an attractive target for potential Alzheimer's disease therapies.

Author contributions: V.B., M.V.P., F.S.G., M.F., and P.G. designed research; V.B., M.V.P., and Y.K. performed research; V.B., M.V.P., and S.C.S. contributed new reagents/analytic tools; V.B., M.V.P., Y.K., F.S.G., M.F., and P.G. analyzed data; and V.B., M.V.P., F.S.G., M.F., and P.G. wrote the paper.

Reviewers: Y.-M.L., Memorial Sloan–Kettering Cancer Center; and S.S.S., The University of Chicago.

The authors declare no conflict of interest.

Freely available online through the PNAS open access option.

See Commentary on page 6885.

[1]To whom correspondence may be addressed. Email: vbustos@rockefeller.edu or greengard@rockefeller.edu.

[2]Present address: Department of Cell and Molecular Biology, Karolinska Institutet, SE-171 77 Stockholm, Sweden.

This article contains supporting information online at www.pnas.org/lookup/suppl/doi:10.1073/pnas.1705235114/-/DCSupplemental.

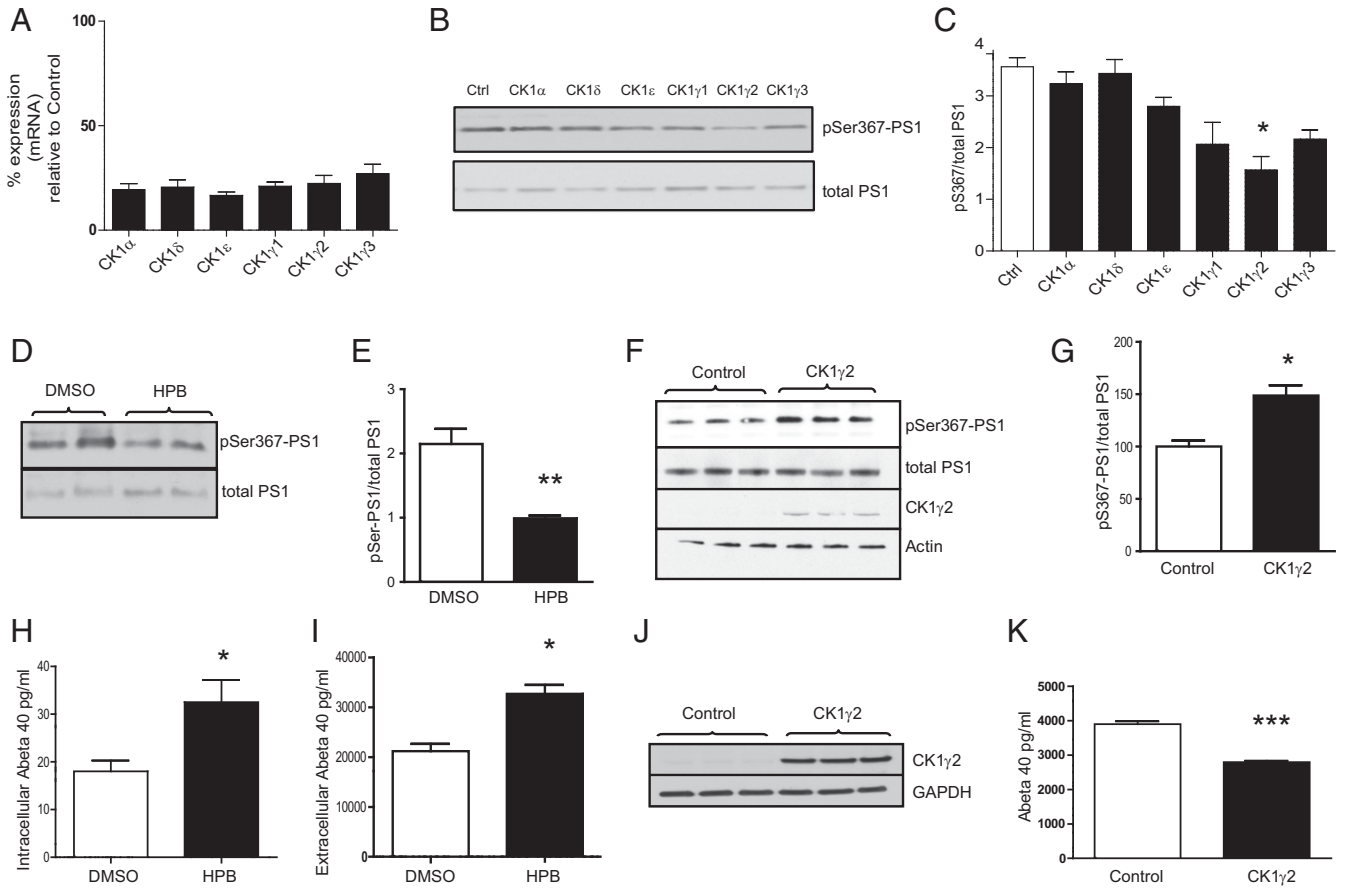

Fig. 1. PS1 is phosphorylated at Ser367 by CK1γ2. (*A*) Analysis of the level of knockdown of the CK1 isoforms by quantitative PCR. $n = 3$. (*B*) Knockdown of CK1γ2 isoform decreases phosphorylation of PS1 at Ser367 in N2A cells. (*C*) Densitometric analysis of pS367/total PS1. $n = 3$. (*D* and *E*) Inhibition of CK1γ decreases PS1-Ser367 phosphorylation. N2A cells were treated for 24 h with 5 μM HPB, a CK1γ-specific inhibitor, resulting in a 57% decrease in the phosphorylation of PS1 at Ser367. $n = 6$. (*F* and *G*) Mouse fibroblasts transfected with CK1γ2 showed a 49% increase in the phosphorylation of PS1 at Ser367. $n = 3$. (*H* and *I*) N2A cells were treated for 12 h with 5 μM HPB, resulting in an increase in intracellular (*H*) and released (*I*) Aβ. $n = 4$. (*J* and *K*) Overexpression of CK1γ2 induces a 33% decrease in Aβ40 in N2A695 cells. $n = 3$. Data represent means ± SEM [$^{*}P < 0.05$, $^{**}P < 0.01$, $^{***}P < 0.001$ compared with control (Ctrl), *t* test].

We next tested the effect of CK1γ inhibition on Aβ levels. Treatment of N2A cells overexpressing APP with HPB induced a 56% increase in intracellular Aβ40 levels (Fig. 1*H*) and a 52% increase in secreted Aβ40 levels (Fig. 1*I*). In addition, overexpression of CK1γ2 in N2A695 cells induced a 33% decrease in Aβ40 (Fig. 1 *J* and *K*), indicating that CK1γ2 activity helps maintain low Aβ levels.

Phosphorylation of PS1 at Ser367 Regulates Aβ Levels in Vivo. To determine whether phosphorylation of PS1-Ser367 affected Aβ metabolism in vivo, we created knock-in transgenic mice where phosphorylation of Ser367 was eliminated by mutation of this residue to Ala (S367A). These mice were crossed with the J20 AD mouse model, which overexpresses human APP containing three mutations linked to familial AD (11). Levels of soluble and insoluble Aβ40 and Aβ42 were each dramatically increased in brains of 9-mo-old J20-S367A transgenic mice (Fig. 2 *A*–*D*). For example, J20-S367A mice had a 40-fold increase in insoluble Aβ40 compared with J20 mice (980 ± SD 338 ng/g of wet tissue versus 24 ± SD 5 ng/g of wet tissue, respectively) (Fig. 2*C*). Immunostaining of brain slices revealed a significant increase in amyloid plaques in the brains of J20-S367A mice (Fig. 2 *E* and *F*). A transgenic mouse line where PS1-Ser367 was mutated to the phosphomimetic Asp (J20-S367D) accumulated the same amounts of Aβ species and amyloid plaques as did J20-S367A (Fig. S1). This finding is consistent with some other phosphomimetic mutants (12–14), in that this mutation did not mimic phosphorylated Ser367, but behaved like the nonphosphorylated PS1-S367A knock-in. We also measured endogenous levels of soluble Aβ40 and Aβ42 in wild-type and PS1-S367A knock-in mice, which express endogenous APP (Fig. 3 *A* and *B*). As observed with the J20-PS1-S367A mice, there was an increase in levels of Aβ40 and Aβ42. These data show that a mutation of PS1-Ser367 to a nonphosphorylatable Ala induces an increase in Aβ levels and amyloid plaque formation in vivo.

PS1-Ser367 Phosphorylation Does Not Affect γ-Secretase Activity. Because PS1 is the subunit of the γ-secretase complex that proteolytically catalyzes the formation of Aβ, the effect of the Ser367 phosphorylation on γ-secretase activity was assessed. For this purpose, we analyzed γ-secretase activity in vitro by using recombinant βCTF-Flag as a substrate and membranes from brains of wild-type (WT) or S367A knock-in mice as a γ-secretase source. Neither the K_m nor V_{max} for βCTF cleavage were affected by the mutation of Ser367 (Fig. 4*A*). To confirm the phosphorylation of PS1 at Ser367 in this assay, we developed an antibody that specifically recognizes PS1 phosphorylated at Ser367 (pSer367), but does not bind nonphosphorylated PS1, pSer365, or pSer366 (Fig. S2 *A* and *B*). After incubation, samples were analyzed for the presence of PS1-pSer367 by immunoblot. Phosphorylated PS1 was detected in membranes from WT mice but not in those from S367A mice (Fig. 4*B*). In these conditions, the stoichiometry of phosphorylation of PS1-Ser367 was 0.65 ± 0.15. WT or PS1-S367A mice expressed

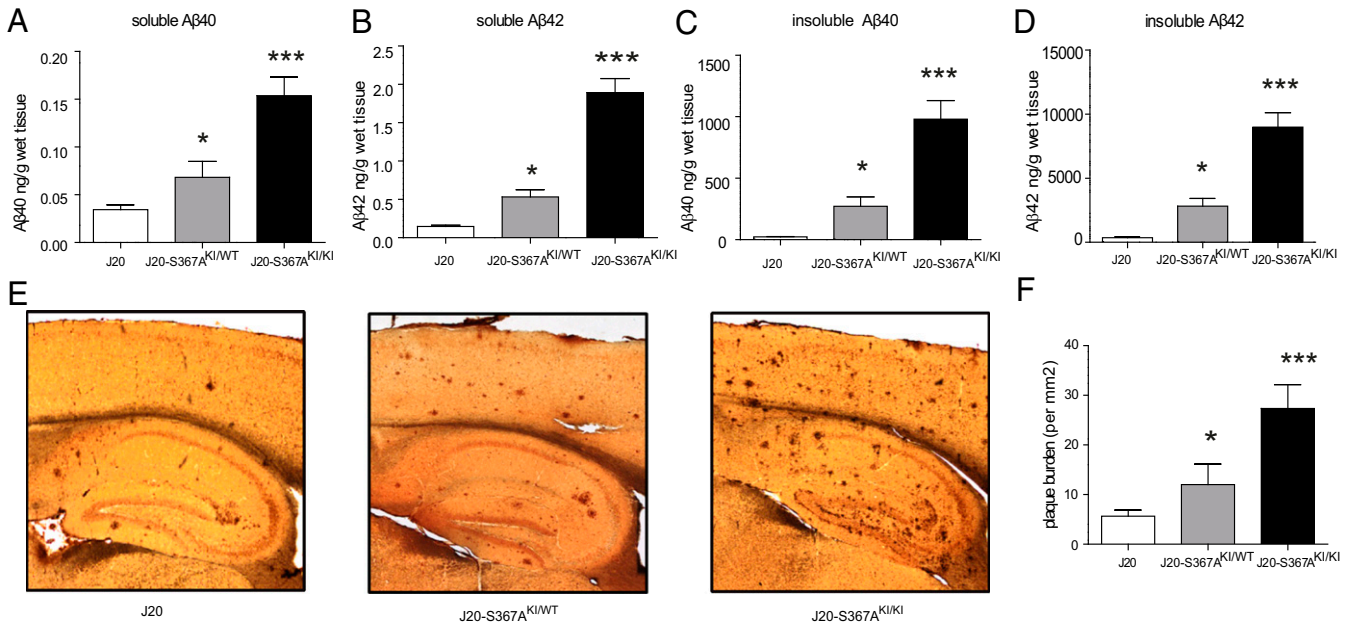

Fig. 2. Phosphorylation of PS1 at Ser367 reduces Aβ levels and plaque burden in brains of Alzheimer's disease model mice. (*A–D*) J20-S367A mice were generated by crossing the J20 Alzheimer model mice to PS1-S367A knock-in (KI) mice. The levels of soluble Aβ40 (*A*), soluble Aβ42 (*B*), insoluble Aβ40 (*C*), and insoluble Aβ42 (*D*), in 9-mo-old mouse brains were analyzed by ELISA. KI/WT refers to mice with the heterozygous mutation, and KI/KI refers to mice with the homozygous mutation. Data represent means ± SEM (J20: $n = 6$; J20-S367AKI/WT: $n = 6$; J20-S367AKI/KI: $n = 6$). (*E*) Amyloid plaques in sections from 9-mo-old J20, J20-S367AKI/WT, and J20-S367AKI/KI mouse brains. (*F*) Quantification of plaque burden. Amyloid plaques were revealed by 6E10 immunostaining. Data represent means ± SEM (J20: $n = 5$; J20-S367AKI/WT: $n = 7$; J20-S367AKI/KI: $n = 6$; $^*P < 0.05$, $^{***}P < 0.001$, ANOVA test).

similar levels of PS1 (Fig. S3). We also analyzed γ-secretase activity by evaluating its ability to bind to a γ-secretase activity-sensing probe (15), which binds only to an active PS1 conformation. Membranes from WT or PS1-S367A mutant mice were incubated with a photoactivatable biotinylated probe. After photoactivation, the reactants were incubated with agarose-streptavidin beads and bound proteins were separated by SDS/polyacrylamide gel electrophoresis (PAGE). The amount of PS1 captured by the beads, a measure of γ-secretase in the active state, was determined by immunoblot (Fig. 4*C*). The results using this activity sensor confirmed those of studies with the βCTF substrate: Mutation of PS1 at Ser367 does not change γ-secretase activity in mouse brain. To further investigate the cause of the dramatic increase in Aβ seen in J20-PS1-S367A mice, we focused on mechanisms independent of its γ-secretase activity.

To determine the effects of phosphorylation of PS1-Ser367 on APP processing, we compared the levels of APP products in brains from WT and PS1-S367A mice. The PS1-S367A mutation caused a significant increase in βCTF levels in vivo (Fig. 4 *D* and *E*), but did not affect the levels of αCTF (Fig. 4 *D* and *F*), soluble APPβ (sAPPβ) (Fig. 4 *D* and *G*), or full-length APP (Fig. 4*D* and *H*). The lack of effect on sAPPβ suggests that the observed increase in βCTF level was not due to increased BACE cleavage of APP. The alternative, that reduced βCTF degradation accounts for the accumulation of βCTF and increased Aβ levels seen in the PS1-S367A mutant mice, was next examined.

The mechanism of the increase in βCTF levels was first investigated in mouse embryonic fibroblasts (MEFs) derived from WT or S367A knock-in mice. To achieve high levels of βCTF expression, we transfected these MEFs with APP harboring the Swedish Alzheimer mutation (APPswe). Pulse–chase experiments with [^{35}S]Methionine indicate that in WT MEFs, the half-life of βCTF was ∼50 min, whereas in MEFs derived from S367A mice, it increased to more than 150 min (Fig. 4 *I* and *J*). These data indicate that the phosphorylation of PS1 at Ser367 decreases the half-life of βCTF by promoting its degradation through a mechanism independent of γ-secretase activity.

PS1 Regulates βCTF Degradation Through Autophagy. To explore the proteolytic pathway involved in βCTF degradation, MEFs derived from WT or PS1-S367A mice were transfected with APPswe, and the autophagic pathway or the proteasome were chemically inhibited. Autophagy inhibition led to an increase in βCTF levels in WT MEFs, but it failed to increase βCTF levels in PS1-S367A MEFs (Fig. 5*A*). Previously, we and others have reported that βCTF is degraded through autophagy (16–18), a sequential process that leads to lysosomal degradation of cellular components.

To further explore a potential relationship between PS1 and autophagy, the levels of the LC3 protein, a marker of autophagic flux, were examined. We observed an increase in LC3-II levels in S367A brains compared with WT brains (Fig. 5 *B* and *C*). LC3-II levels can increase as a result of increased autophagy or its decreased lysosomal degradation. To differentiate between these two possibilities, we examined the levels of SQSTM1/p62, a marker of lysosomal protein degradation. We observed an increase similar to

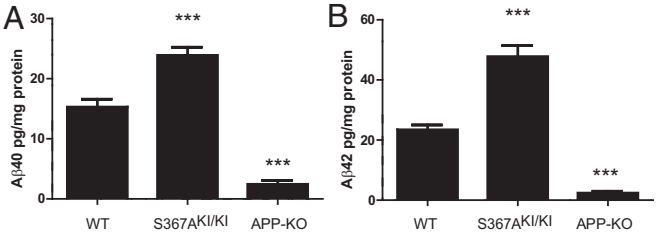

Fig. 3. Phosphorylation of PS1 at Ser367 reduces Aβ levels in brains expressing endogenous levels of APP. Endogenous Aβ40 (*A*) and Aβ42 (*B*) are increased in the brains of knock-in PS1-S367A mice compared with wild-type mice. $n = 7$; $^{***}P < 0.001$, ANOVA test.

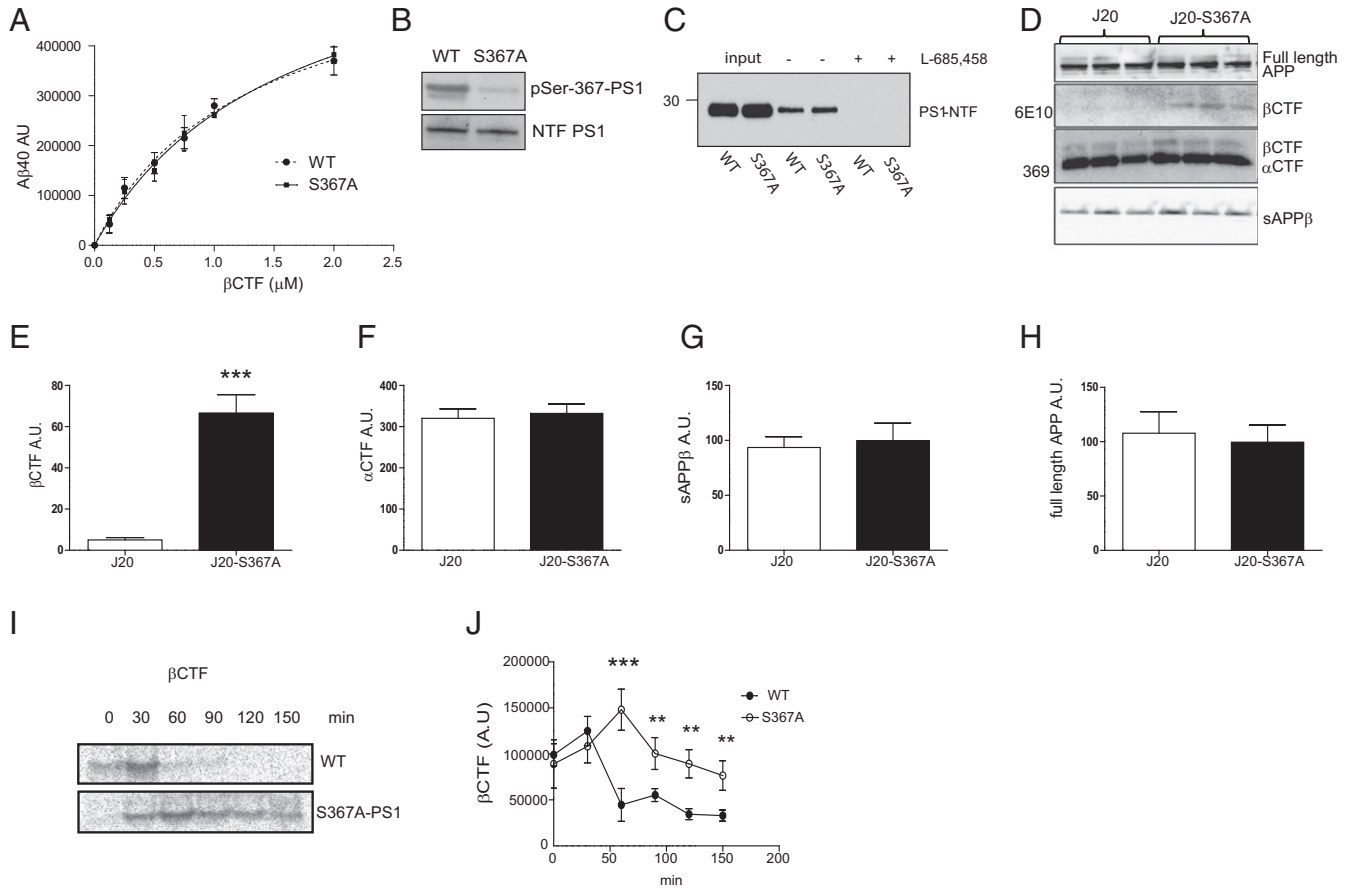

Fig. 4. βCTF degradation is increased by the phosphorylation of PS1 at Ser367. (*A*) In vitro γ-secretase activity assay. Indicated concentrations of βCTF-Flag were added to CHAPSO-solubilized brain membranes derived from WT or S367A knock-in mice. After 90 min, aliquots were assayed for Aβ40 by ELISA. Aβ40 levels are expressed as arbitrary units. $n = 3$. (*B*) Solubilized brain membranes used in *A* are phosphorylated at PS1-Ser367. (*C*) Analysis of active γ-secretase levels. Membranes isolated from brains of WT or S367A mutant mice were incubated with JC-8 (a photoactivatable γ-secretase probe), photolysed, pulled down with streptavidin beads, and subject to immunoblot analysis using PS1-NTF antibody. Addition of L-685,458, a γ-secretase inhibitor, blocks the binding of JC-8 to γ-secretase, indicating binding specificity. $n = 3$. (*D–H*) Levels of βCTF were increased in the brains of J20-S367A knock-in mice compared with J20 mice (*D* and *E*), but no changes were observed in the levels of αCTF (*D* and *F*), sAPPβ (*D* and *G*), or full-length APP (*D* and *H*). (*I* and *J*) Fibroblasts derived from WT or S367A knock-in mice were transfected with APPswe and subject to pulse–chase analysis for the indicated time points. $n = 3$. Data represent means ± SEM (**$P < 0.01$, ***$P < 0.001$; *t* test for *E* and ANOVA test for *J*).

LC3-II in SQSTM1/p62 levels in S367A brains compared with WT brains (Fig. 5 *B* and *D*). This increase was also seen in isolated cultured cortical neurons (Fig. 5 *E* and *F*). The increase in the levels of both LC3-II and SQSTM1/p62 suggests impaired autophagic flux. To demonstrate the role of PS1 phosphorylation in autophagic flux, MEF derived from WT or PS1-S367A knock-in mice were transfected with GFP-RFP-LC3, and the colocalization between GFP and RFP was measured in conditions of normal media, without serum and without serum plus the lysosomal inhibitor, bafilomycin. The result demonstrates that phosphorylation of PS1-Ser367 regulates autophagic flux (Fig. 5 *G* and *H*).

In summary, our results show that lack of PS1-Ser367 phosphorylation reduces autophagic flux, causing the accumulation of βCTF, which in turn leads to increased Aβ levels.

Discussion

Presenilin 1 is an intramembrane protease, harboring the catalytic site of the γ-secretase complex. Although PS1 has a central role in the generation of β-amyloid, little is known about other possible functions. Here, we describe a phosphorylation site on PS1 that regulates autophagy and promotes the degradation of βCTF. Mutation of the phosphorylatable Ser367 of PS1 to Ala led to a dramatic increase in Aβ levels in vivo. Two independent assays demonstrated that the Ser367 to Ala mutation did not modify γ-secretase activity. Consistent with our results and conclusions, others recently reported that 15 phosphorylation sites in PS1, including Ser367, did not affect the assembly, maturation, and activity of γ-secretase, using highly purified γ-secretase in an in vitro assay (19).

Phosphomimetic mutations are commonly used to test the functional consequences of protein phosphorylation. However, a direct comparison between the phosphorylation mimics and the corresponding phosphorylated form of the protein is rarely carried out. Our in vivo studies demonstrate that the phosphomimic S367D does not reproduce the effect of phosphorylation on Aβ metabolism, indicating that the full charge and geometry of a phosphate group is required for its effect.

Recently, it was reported that the PS1-S367D mutation induced a closed conformation in cells, as was also seen in PS1 containing familial Alzheimer's disease mutations (20). The authors concluded, based on the assumption that the Asp mutation mimics phosphorylation, that phosphorylation at PS1-Ser367 was pathogenic (21). In contrast, in our work, we have demonstrated that the S367D mutation does not mimic PS1 phosphorylation because it induces the same Aβ accumulation as the S367A mutation. Therefore, we conclude that phosphorylation of PS1 at Ser367 is

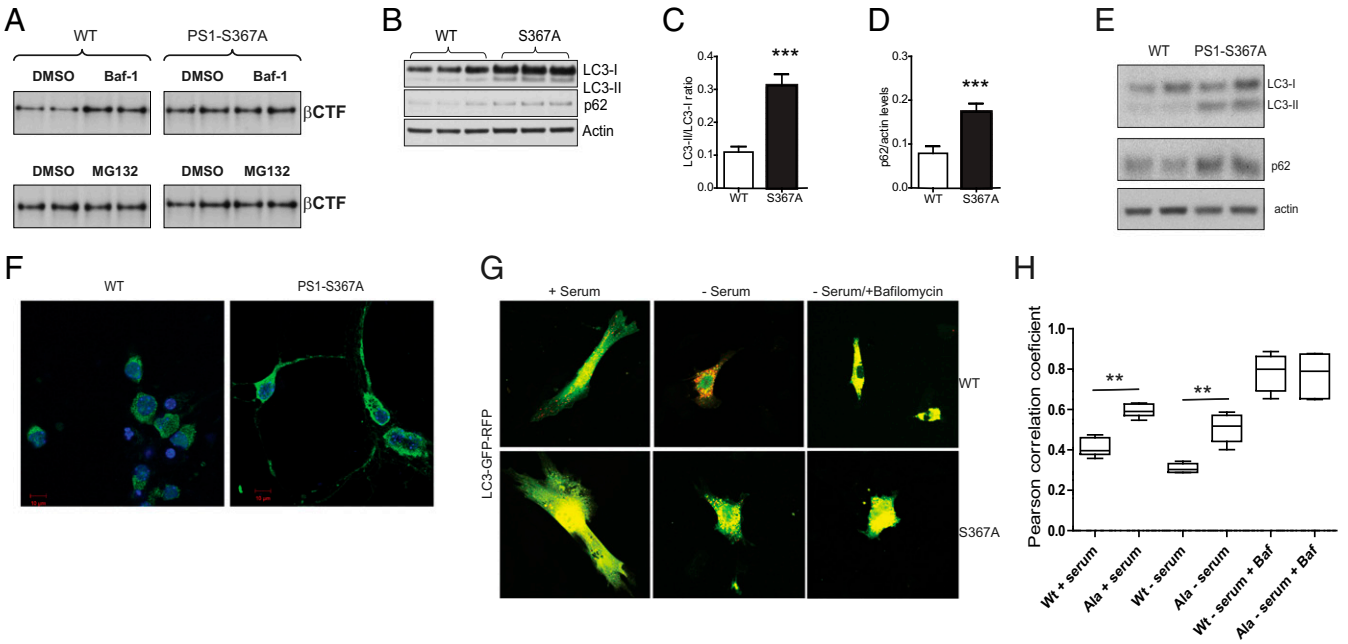

Fig. 5. Autophagy is regulated by the phosphorylation of PS1 at Ser367. (*A*) MEFs derived from WT or PS1-S367A were transfected with APPswe. In *Upper*, autophagy was inhibited by incubating with 10 nM Bafilomycin a1 for 3 h. In *Lower*, the proteasome was inhibited by incubating with 10 μM MG132 for 8 h. Cell lysates were immunoblotted with the 6E10 antibody to detect βCTF. (*B–D*) LC3-II and SQSMT1/p62 levels were elevated in the brains of S367A knock-in mice compared with WT mice as measured by analysis of immunoblots. In *B*, results from three different WT and S367A mutant mice are shown. (*E*) Immunoblot against LC3 and p62 from lysates prepared from WT or PS1-S367A cultured neurons. (*F*) Immunofluorescence against LC3 (green) and DAPI (blue) in WT and PS1-S367A neurons in culture. (*G*) Tandem GFP-RFP-LC3 in MEFs derived from WT or PS1-S367A mice. (*H*) Pearson's correlation coefficient was used as a measure of colocalization of RFP and GFP signals. $n = 20$. Data represent means ± SEM (**$P < 0.01$, ***$P < 0.001$).

protective, a conclusion consistent with all of the other data in this report.

Previously, our laboratory reported that CK1 epsilon increased Aβ production. Here, we find that CK1γ2 appears to be the physiological kinase phosphorylating PS1 at Ser367, suggesting that different CK1 isoforms participate in Aβ metabolism (22). The mechanism by which CK1 epsilon regulates Aβ metabolism remains to be investigated.

In the PS1-S367A mutant line, we observed an accumulation of βCTF without changes in the levels of total APP, sAPPβ, or αCTF. The differential susceptibility of βCTF and αCTF to autophagic degradation could be due to differences in their site of synthesis. Although βCTF is synthesized in endosomes and autophagic vesicles, αCTF synthesis occurs predominantly on the cell surface, rendering it less prone to undergo autophagic degradation.

Recently, the effect of PS1 familial Alzheimer's disease (FAD) mutations on highly purified γ-secretase activity was reported (23). Interestingly, many mutations, which have been shown to increase the amount of Aβ peptides in vivo, were shown to decrease γ-secretase activity in vitro. Further work should characterize the impact of Presenilin 1 FAD mutations on PS1-Ser367 phosphorylation and on the autophagic degradation of βCTF.

Our results demonstrate that PS1 regulates Aβ levels in a bi-directional manner. Thus, in addition to its known role as the catalytic subunit of the γ-secretase complex, through which it converts βCTF to Aβ, selective phosphorylation of PS1 on Ser367 decreases Aβ levels by increasing βCTF degradation through autophagy. Elucidation of the mechanisms that regulate PS1 phosphorylation at Ser367 should aid in the development of potential therapies for Alzheimer's disease.

Methods

In Vitro Phosphorylation Assays. In vitro assays were performed in a final volume of 50 μL in the following conditions: 50 mM Hepes pH 7.4, 150 mM NaCl, 10 mM $MgCl_2$, 1 mM [γ^{32}P] ATP (1,000 cpm/pmol), 1 μg of GST-protein or 1 μg of casein as a control, and 100 ng of protein kinase CK1γ (Sigma). Reactions were performed at 30 °C for 10 min. Samples were analyzed by SDS/PAGE and autoradiography.

Protein Quantification and Immunoblot Analysis. Cultured cells or brain tissues were lysed in buffer A (50 mM Tris·HCl, pH 7.5, 150 mM NaCl, and 2 mM MgCl) supplemented with 1% Triton X-100, a protease inhibitor mixture (Complete-EDTA free; Roche) and phosphatase inhibitors (30 mM NaF, 1 mM orthovanadate, and 30 mM pyrophosphate). The cell or tissue lysates were disrupted with a probe-type sonicator for 10 s twice, centrifuged, and the protein levels in the supernatant measured by the BCA method. For Aβ40, Aβ42, and sAPPβ, conditioned cell culture media were analyzed. The samples were boiled in standard protein sample buffer, and subjected to SDS/PAGE followed by protein transfer onto a PVDF membrane and incubated overnight at 4 °C with the following antibodies: anti-PS1 (mouse monoclonal, 1:1,000; EMD Millipore), anti-APP (6E10, mouse monoclonal, 1:1,000; Covance) for total APP and βCTF, anti-actin (rabbit polyclonal, 1:1,000; Santa Cruz), anti-LC3 (rabbit polyclonal, 1:1,000; Sigma), anti-p62 (rabbit polyclonal, 1:500; Cell Signaling Technology), anti-CK1γ2 (rabbit polyclonal 1:500; Abcam), anti–PS1-NTF (a polyclonal antibody generated in our laboratory), and anti-sAPPβ (a polyclonal antibody generated in our laboratory).

ELISA for Aβ. The quantitative analysis of Aβ40 or Aβ42 was performed by using an ELISA kit according to the manufacturer's instructions (Life Technologies). Briefly, supernatants of conditioned media from N2A/APP695 cells were diluted in buffer and incubated in a 96-well plate with Aβ40 or Aβ42 antibody for 3 h at room temperature. After washes of unbound material, a secondary antibody conjugated to horseradish peroxidase (HRP) was added for 30 min. Unbound secondary antibody was washed, and subsequently samples were incubated with a developing reagent for 30 min. Stop solution was added to block further reaction between HRP and the colorimetric substrate. An absorbance multiplate reader was used to quantify the colorimetric reaction at 450 nm.

Cell Culture and Transfection. Mouse N2A neuroblastoma WT cells and an established N2A cell line expressing APP695 were maintained in medium containing 50% DMEM and 50% Opti-MEM, supplemented with 5% FBS and 200 μg/mL G418 (Life Technologies). These cells line were tested for

mycoplasma contamination by using LookOut mycoplasma PCR detection (Sigma). Transient transfection of plasmid encoding CK1γ2 or APPsw was performed by using FuGENE 6 (Roche) or Lipofectamine 2000 (Life Technologies). Compound HPB (5 μM, synthesized in house following the methodology described in ref. 10), β-secretase inhibitor IV (10 μM), and γ-secretase inhibitor DAPT (5 μM) were incubated for the indicated times.

In Vitro γ-Secretase Assay. Membranes containing γ-secretase were prepared from brains of WT, S367A, or S367D mice and solubilized in 2% CHAPSO. γ-Secretase membranes were incubated with substrate βCTF-FLAG for 90 min, and Aβ40 levels were measured by ELISA.

Brain Aβ Measurement. For the analysis of mouse brains, mice were euthanized by CO_2 followed by decapitation. Brains were removed and frozen on dry ice and stored at −80 °C until use. Half brains were homogenized in TBS containing protease inhibitor mixture (Roche). The homogenized brains were centrifuged at 300,000 × *g* for 30 min. The supernatants were used to measure the levels of soluble Aβ40 and Aβ42. The pellets were suspended in 70% formic acid and sonicated for 30 s. The samples were neutralized in 10 volumes of neutralization buffer (1 M Tris-base, 0.5 M Na_2HPO_4, 0.05% NaN_3 pH 9.0), and insoluble Aβ40 and Aβ42 were measured by ELISA.

Stoichiometry of Phosphorylation. The stoichiometry of phosphorylation was determined by comparing PS1 phosphorylated at Ser367 from brain membranes with phosphorylated recombinant PS1-third intracellular loop fused to GST. To calculate the stoichiometry of phosphorylation of GST-PS1, 5.0 pmoles of GST-PS1 were phosphorylated with 1.0 pmol of CK1γ2 in 50 mM Hepes (pH 7.4), 150 mM NaCl, 10 mM $MgCl_2$, 100 μM ATP, 1 μCi [γ-^{32}P] ATP at 30 °C for 30 min. The phosphorylated GST-PS1 was separated by SDS/PAGE (10–20% Tricine; Invitrogen). The total amount of GST-PS1 was quantified by SDS/PAGE with Coomassie staining by using BSA as standard. Phosphate incorporation was quantified by using a scintillation counter (Beckman LS6500). The stoichiometry of GST-PS1 phosphorylation was calculated by ^{32}P incorporation in relation to total protein. By using phosphorylated GST-PS1 as a standard, quantitative immunoblotting was performed for PS1 phosphorylated at Ser367 from brain membranes.

Immunofluorescence. For immunofluorescence microscopy, cells were fixed in 4% paraformaldehyde or ice-cold methanol for 10 min, permeabilized in 0.2% Triton in PBS (PBST), and blocked in 10% donkey serum for 1 h at room temperature. Cells were then incubated with primary antibody overnight at 4 °C, washed five times in PBST, and incubated with secondary antibody for 1 h at room temperature. Cells were mounted by using Vectashield mounting medium with DAPI (Vector Laboratories) and analyzed by using a Zeiss LSM710 laser confocal microscope.

Immunohistochemistry. The brains of 9-mo-old J20, J20-PS1-367A, or J20-PS1-S367D mice were processed, embedded, and sectioned at 40 μm. For amyloid plaque quantification, the blocks were serial sectioned across the whole hippocampus, and every eighth section was used for staining (~20 sections per animal). Briefly, free-floating sections were incubated in 0.3% H_2O_2 for 15 min to block endogenous peroxidase activity, and then incubated in a mouse-on-mouse (MOM) blocking reagent from the MOM immunodetection kit (Vector Laboratories) to block nonspecific binding, followed by incubation in a MOM diluent containing 6E10 primary antibody at room temperature for 30 min, then reacted with MOM biotinylated anti-mouse IgG reagent (1:2,000) for 10 min. Antibody labeling was detected by using Vectastatin ABC kit (Vector Laboratories). The amyloid plaque load density in the cortex and the hippocampal region was manually counted by using ImageJ software.

Animals. All procedures involving animals were approved by The Rockefeller University Institutional Animal Care and Use Committee and were in accordance with the National Institutes of Health guidelines. J20 mice were purchased from The Jackson Laboratory. PS1 S367A and PS1 S367D are constitutive knock-ins in C57BL/6J mice and were generated by homolog recombination targeting exon 10. We produced the progeny by using in vitro fertilization and embryo transfer techniques to generate the number of animals needed for the biochemical tests. Only male animals were used in this study.

Statistical Analysis. The data are presented as means ± SEM. Unless otherwise mentioned, the data are based on three independent experiments. The significance level was determined by using a two-tailed Student's *t* test, as indicated in the figure legends. For analysis of the statistical significance of differences between more than two groups, we performed repeated measures one-way ANOVA tests with a 95% confidence interval. All statistical analyses were performed by using GraphPad Prism software. No randomization or blinding was used, and no animals were excluded from analysis. Sample sizes were selected on the basis of previous publications.

ACKNOWLEDGMENTS. We thank Dr. Yotam Sagi and Dr. Jean-Pierre Roussarie for constructive discussion, the transgenic services resource center for mouse in vitro fertilization, and H. Molina for peptide synthesis. This work was supported by the Fisher Center for Alzheimer's Research Foundation, National Institutes of Health Grant AG047781, Department of Defense/US Army Medical Research Acquisition Activity (DOD/USAMRAA) Grant W81XWH-09-1-0402, and JPB Foundation Grant 475 (to P.G.). V.B. was supported by DOD/USAMRAA Grant W81XWH-14-1-0045. S.C.S. was supported by JPB Foundation Grant 322. F.S.G. was supported by DK098109 and a Veterans Affairs Merit Award.

1. Hardy J, Selkoe DJ (2002) The amyloid hypothesis of Alzheimer's disease: progress and problems on the road to therapeutics. *Science* 297:353–356.
2. Cai H, et al. (2001) BACE1 is the major β-secretase for generation of Abeta peptides by neurons. *Nat Neurosci* 4:233–234.
3. De Strooper B, et al. (1998) Deficiency of presenilin-1 inhibits the normal cleavage of amyloid precursor protein. *Nature* 391:387–390.
4. Prager K, et al. (2007) A structural switch of presenilin 1 by glycogen synthase kinase 3β-mediated phosphorylation regulates the interaction with β-catenin and its nuclear signaling. *J Biol Chem* 282:14083–14093.
5. Lau K-F, et al. (2002) Cyclin-dependent kinase-5/p35 phosphorylates Presenilin 1 to regulate carboxy-terminal fragment stability. *Mol Cell Neurosci* 20:13–20.
6. Fluhrer R, Friedlein A, Haass C, Walter J (2004) Phosphorylation of presenilin 1 at the caspase recognition site regulates its proteolytic processing and the progression of apoptosis. *J Biol Chem* 279:1585–1593.
7. Sannerud R, et al. (2016) Restricted location of PSEN2/γ-secretase determines substrate specificity and generates an intracellular Aβ pool. *Cell* 166:193–208.
8. Dephoure N, et al. (2008) A quantitative atlas of mitotic phosphorylation. *Proc Natl Acad Sci USA* 105:10762–10767.
9. Xue Y, et al. (2008) GPS 2.0, a tool to predict kinase-specific phosphorylation sites in hierarchy. *Mol Cell Proteomics* 7:1598–1608.
10. Hua Z, et al. (2012) 2-Phenylamino-6-cyano-1H-benzimidazole-based isoform selective casein kinase 1 gamma (CK1γ) inhibitors. *Bioorg Med Chem Lett* 22:5392–5395.
11. Mucke L, et al. (2000) High-level neuronal expression of abeta 1-42 in wild-type human amyloid protein precursor transgenic mice: synaptotoxicity without plaque formation. *J Neurosci* 20:4050–4058.
12. Vandel L, Kouzarides T (1999) Residues phosphorylated by TFIIH are required for E2F-1 degradation during S-phase. *EMBO J* 18:4280–4291.
13. Paleologou KE, et al. (2008) Phosphorylation at Ser-129 but not the phosphomimics S129E/D inhibits the fibrillation of α-synuclein. *J Biol Chem* 283:16895–16905.
14. Chang SS, et al. (2017) Aurora A kinase activates YAP signaling in triple-negative breast cancer. *Oncogene* 36:1265–1275.
15. Chau D-M, Crump CJ, Villa JC, Scheinberg DA, Li Y-M (2012) Familial Alzheimer disease presenilin-1 mutations alter the active site conformation of γ-secretase. *J Biol Chem* 287:17288–17296.
16. Jaeger PA, et al. (2010) Regulation of amyloid precursor protein processing by the Beclin 1 complex. *PLoS One* 5:e11102.
17. Tian Y, Bustos V, Flajolet M, Greengard P (2011) A small-molecule enhancer of autophagy decreases levels of Abeta and APP-CTF via Atg5-dependent autophagy pathway. *FASEB J* 25:1934–1942.
18. Tian Y, Chang JC, Fan EY, Flajolet M, Greengard P (2013) Adaptor complex AP2/PICALM, through interaction with LC3, targets Alzheimer's APP-CTF for terminal degradation via autophagy. *Proc Natl Acad Sci USA* 110:17071–17076.
19. Matz A, et al. (2015) Identification of new Presenilin-1 phosphosites: Implication for γ-secretase activity and Aβ production. *J Neurochem* 133:409–421.
20. Berezovska O, et al. (2005) Familial Alzheimer's disease presenilin 1 mutations cause alterations in the conformation of presenilin and interactions with amyloid precursor protein. *J Neurosci* 25:3009–3017.
21. Maesako M, et al. (2017) Pathogenic PS1 phosphorylation at Ser367. *eLife* 6:e19720.
22. Flajolet M, et al. (2007) Regulation of Alzheimer's disease amyloid-β formation by casein kinase I. *Proc Natl Acad Sci USA* 104:4159–4164.
23. Sun L, Zhou R, Yang G, Shi Y (2016) Analysis of 138 pathogenic mutations in presenilin-1 on the in vitro production of Aβ42 and Aβ40 peptides by γ-secretase. *Proc Natl Acad Sci USA* 114:E476–E485.